*Article*

# Dynamic Simulation Model of Miniature Tracked Forestry Tractor for Overturning and Rollover Safety Evaluation

Yun-Jeong Yang [1,2], Moon-Kyeong Jang [1,2] and Ju-Seok Nam [1,2,*]

[1] Department of Biosystems Engineering, Kangwon National University, 1 Kangwondaehak-gil, Chuncheon 24341, Gangwon-do, Republic of Korea; yyj000501@naver.com (Y.-J.Y.); moon2842@naver.com (M.-K.J.)

[2] Interdisciplinary Program in Smart Agriculture, Kangwon National University, 1 Kangwondaehak-gil, Chuncheon 24341, Gangwon-do, Republic of Korea

* Correspondence: njsg1218@kangwon.ac.kr; Tel.: +82-33-250-6497

**Abstract:** This study proposes a method to construct a dynamic simulation model to implement the lateral overturning and backward rollover characteristics of an actual tractor. Based on theoretical analysis, factors affecting these characteristics are identified, which include tractor weight, track width, wheelbase, location of mass center, weight distribution, heights of front and rear axles, and geometric shapes. The location of the mass center of the actual tractor is measured based on the standard test procedure set by the International Organization for Standardization, and the remaining influencing factors are derived through measurements. A three-dimensional (3D) model of the tractor is constructed to reflect all these factors. Additionally, a simulation model utilizing this 3D model is developed using a commercial dynamic simulation software program. The ability of the model to simulate the overturning and rollover characteristics of the actual tractor is verified by comparing the static sidelong falling angle and minimum turning radius with those of the actual tractor. The errors between the characteristics of the actual tractor and those of the 3D model and dynamic simulations are shown to be less than 5%, thus indicating that the proposed method can effectively simulate the overturning and rollover characteristics of the actual tractor.

**Keywords:** dynamic simulation model; miniature tracked forestry tractor; minimum turning radius; overturning; rollover; static sidelong falling angle

## 1. Introduction

Owing to the widespread use of agricultural machinery and the aging population of farmers, agricultural accidents have increased [1]. The rate of agricultural accidents is approximately 1.4 times higher than the average for all industries [2], with machinery-related accidents presenting the highest incidence and mortality rates among all industrial accidents [3]. In South Korea, tractors are predominantly responsible for agricultural machinery accidents [4], with overturning and rollover accidents constituting 32% of all such accidents [5]. In the United States, tractor accidents claim over 800 lives annually, with more than half of these accidents involving overturns or rollovers [6]. In Italy, 57.4% (205 cases) of 357 tractor accidents recorded between 2002 and 2012 were caused by overturning and rollover [7]. To address the global increase in tractor overturning/rollover accidents, researchers have intensively investigated tractor safety.

Previati et al. [8] analyzed the effect of ground slope angle, tire stiffness, and tractor axle position on the backward rollover of tractors on slope. They discovered that the slope angle at which backward rollover occurs increases by more than 70% for tractors equipped with front-axle suspension compared with standard tractors. Franceschetti et al. [9] analyzed the effects of tractor weight, track width, and mass center height on lateral overturning. They concluded that lateral overturning is not significantly affected by tractor weight and that safety decreases when the tractor is loaded, owing to the elevated

center of mass. Lee et al. [10] theoretically analyzed the lateral overturning and backward rollover safety of small off-road vehicles to understand the manner in which these safety factors vary with the steering angle during operation.

The lateral overturning and backward rollover safety of agricultural machinery have been extensively investigated through dynamic simulation, which is a method that requires lower cost and time compared with experimental studies [11]. For instance, Shim et al. [12] analyzed the effects of driving direction and ground slope on the lateral overturning of forestry vehicles via dynamic simulation. They revealed that driving in the contour direction on slopes improved safety compared with driving along the slope direction; subsequently, they derived safe driving conditions based on the driving direction. Similarly, Kang et al. [13] performed a simulation to determine the maximum safe slope for driving a red pepper harvester and the critical angle for its backward rollover during collisions; they further suggested considering operating conditions such as crop loading and driver type in future studies. Iqbal et al. [14] performed a dynamic simulation to obtain the ground slope angle at which lateral overturning and backward rollover occur during red pepper transplanting, which provided valuable insights for safety measures. Park et al. [15] performed simulations for forestry forwarders to ascertain the critical speed for lateral overturning under different conditions, such as log loading and slope variations. They suggested reducing its driving speed by approximately 20%, as the increased mass center height decreases lateral overturning safety for a forwarder loaded with logs. Qin et al. [16] performed simulations to analyze the effects of electric power steering (EPS) on the lateral overturning and backward rollover of a tractor. They implemented an irregular road surface, which reflects actual farmland, and adjusted the ground slope angle and tractor speed as variables. The results showed that the EPS improved the lateral overturning and backward rollover safety when the tractor traveled at speeds exceeding 6 m/s on a 15° slope. They highlighted that further research is required to ensure safety on relatively harsh roads.

Whereas many studies have evaluated overturning and rollover safety through simulations, performing tests on actual machinery remains challenging owing to the risks and complexities of implementing tests under varying conditions [17]. Simulations offer a safer and more accessible alternative compared with actual experiments; however, they may not accurately reflect the physical properties of real-world scenarios, thus potentially resulting in significant inaccuracies [18]. Previous studies typically focused on the qualitative effects of key factors on safety, with few models accurately reflecting actual physical properties. Thus, this study proposes a method for constructing a dynamic simulation model to accurately represent the overturning and rollover characteristics of actual tractors. Influential factors are derived through theoretical analysis, and the model is validated via tests that consider the static sidelong falling angle and minimum turning radius. The proposed approach balances accuracy and efficiency. The results from this study are expected to serve as valuable reference data for constructing simulation models for agricultural tractors.

## 2. Materials and Methods

### 2.1. Tractor Overturning and Rollover Theory

Theoretical analysis was conducted via a literature review to determine variables that affect the lateral overturning and backward rollover of a tractor. It was conducted based on wheeled tractors, as references for tracked tractors are not available. For this analysis, the tractor was assumed to be in static equilibrium, with all elements except for the wheels regarded as rigid bodies. Owing to the typically low driving speeds of tractors, air resistance during movement was disregarded [19].

2.1.1. Lateral Overturning on Slope Under Stationary Condition

Figure 1 shows a simplified diagram of a tractor and a free-body diagram for a theoretical analysis of the slope angle at which lateral overturning occurs when the tractor is stopped on a slope [20].
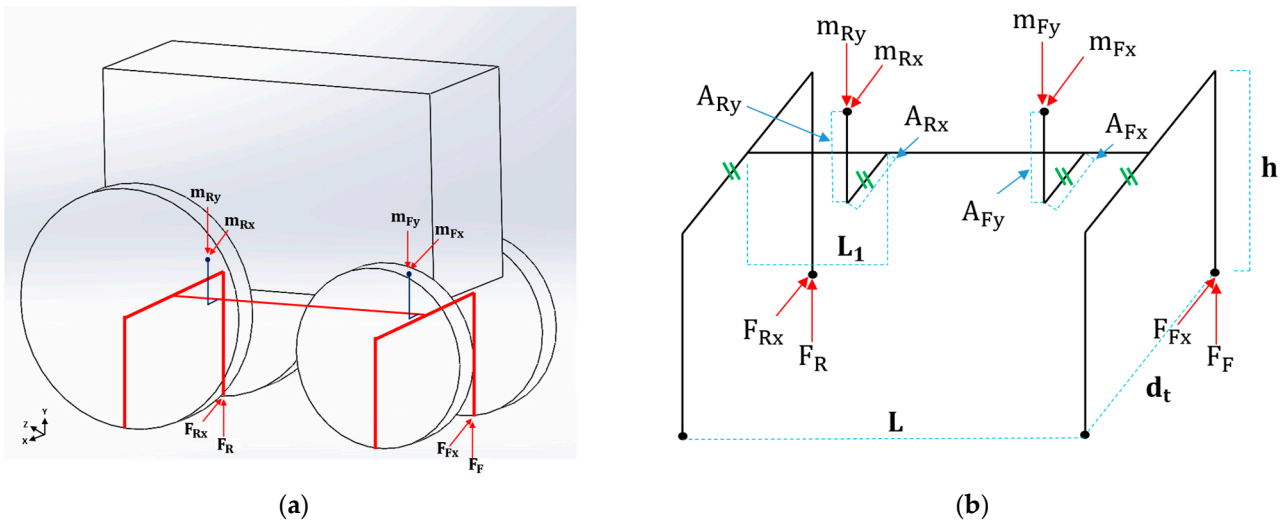
**Figure 1.** Diagram for lateral overturning analysis under stationary condition: (**a**) simplification of tractor model; (**b**) geometric parameters of tractor model.

When the tractor is stopped in the contour direction on a slope, the ground contact forces of the upslope rear wheel and front wheel, $F_R$ and $F_F$, respectively, can be expressed, as shown in Equations (1) and (2), respectively [21].

$$F_R = \frac{m_R g}{d_t} \left[ \frac{L_1}{L} \left( h \sin\theta - \frac{d_t}{2} \cos\theta \right) - (h + A_{Ry}) \sin\theta + \left( \frac{d_t}{2} + A_{Rx} \right) \cos\theta \right], \quad (1)$$

where $F_R$ is the contact force of the rear upslope wheel in the stationary state, $m_R$ is the mass of the tractor at the rear section, g is the gravitational acceleration, $d_t$ is the track width, L is the wheelbase, $L_1$ is the distance from the rear axle to the rear mass center, h is the front-axle height, $\theta$ is the ground slope angle, $A_{Rx}$ is the downslope distance of the rear mass center with respect to the midplane, and $A_{Ry}$ is the height of the rear mass center from the rear axle.

$$F_F = \frac{m_R g}{d_t} \left( \frac{L_1}{L} \right) \left[ \frac{d_t}{2} \cos\theta - h \sin\theta \right] + \frac{m_F g}{d_t} \left[ \left( \frac{d_t}{2} - A_{Fx} \right) \cos\theta - (h_1 + A_{Fy}) \sin\theta \right], \quad (2)$$

where $F_F$ is the contact force of the front upslope wheel in the stationary state, $m_F$ is the mass of the tractor at the front section, $A_{Fx}$ is the downslope distance of the front mass center with respect to the midplane, and $A_{Fy}$ is the height of the front mass center from the front axle.

The contact force between the tractor tire and ground is derived based on the geometric structure of the tractor, its overall mass distribution, and the ground slope. As the ground slope increases, the upslope rear wheel lifts off the ground first, thus initiating a Phase I rollover. If the slope continues to increase, then the upslope front wheel lifts, thus resulting in lateral overturning. The slope angle at which lateral overturning begins due to the zero ground contact force of the rear wheel, $\theta_{R0}$, can be derived by setting $F_R$ to zero in Equation (1), as shown in Equation (3) [21].

$$\theta_{R0} = \tan^{-1} \left( \frac{d_t(L - L_1) - 2A_{Rx}L}{2[(h + A_{Ry})L - hL_1]} \right), \quad (3)$$

where $\theta_{R0}$ is the ground slope angle when the upslope rear wheel begins to lift from the ground.

In Equation (3), variables $L_1$, $A_{Rx}$, and $A_{Ry}$ are related to the location of the mass center. The track width, wheelbase, front-axle height, and mass center of the tractor significantly affect lateral overturning under stationary conditions on a slope.

2.1.2. Lateral Overturning During Constant-Speed Turning

Figure 2 shows a diagram for the theoretical analysis of lateral overturning caused by a turning tractor [19].
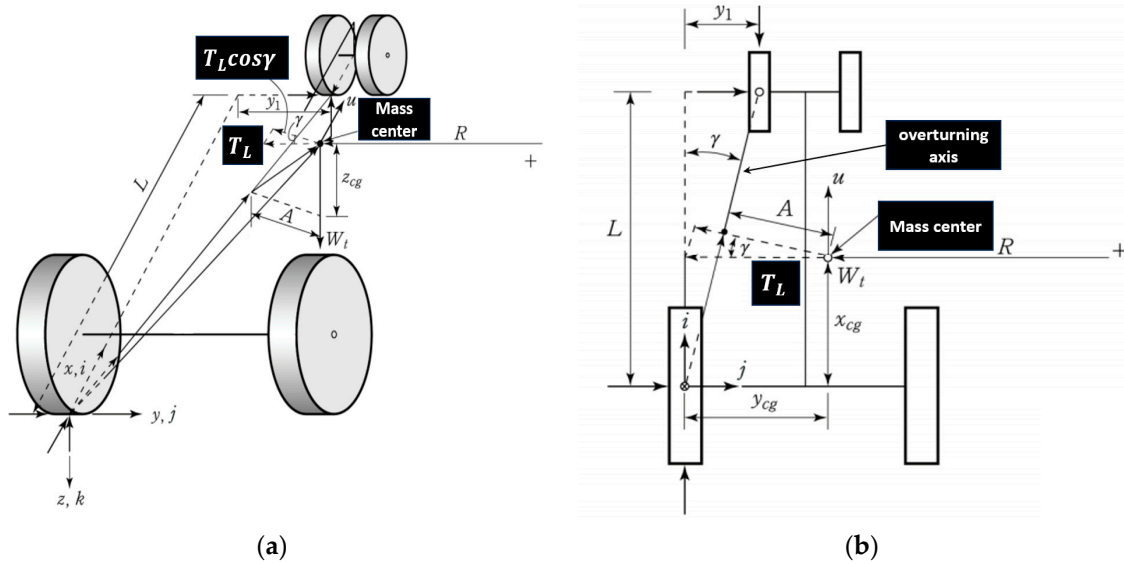


(**a**)                                        (**b**)

**Figure 2.** Diagram for lateral overturning analysis under constant-speed turning: (**a**) isometric view; (**b**) top view.

When a tractor turns at a driving speed of u along a path of radius R, the lateral force exerted on the mass center of the tractor by the wheels can be obtained using Equation (4). As the driving speed increases, the lateral force at the mass center increases as well, which creates a moment about the overturning axis connecting the left front wheel to the ground contact point of the rear wheel, thereby resulting in lateral overturning. If the speed at which the right wheel begins lifting due to lateral overturning is defined as the critical speed $u_s$, then the moment equilibrium for the overturning axis is expressed as shown in Equation (5) [19].

$$T_L = m_t \frac{u^2}{R}, \tag{4}$$

where $T_L$ is the lateral force of the mass center of the tractor, $m_t$ is the tractor mass, u is the travel speed of the tractor, and R is the turning radius of the tractor.

$$m_t \frac{u_s^2}{R} \cos\gamma \, z_{cg} - W_t A = 0, \tag{5}$$

where $\gamma$ is the angle between the lateral force of the mass center and the plane normal to the overturning axis ($\tan^{-1}\left(\frac{y_1}{L}\right)$), $z_{cg}$ is the mass center height of the tractor, $u_s$ is the critical travel speed of the tractor under constant-speed turning, $W_t$ is the tractor weight, and *A* is the normal distance between the mass center and overturning axis.

In Equation (5), the variable A can be determined by considering the location of the mass center ($x_{cg}$, $y_{cg}$, and $z_{cg}$), the wheelbase (L), and the horizontal distance between the centers of the front and rear wheels ($y_1$) [19]. The horizontal distance between the centers of the front and rear wheels is affected by the track width between the front and rear wheels. Therefore, the variables affecting the critical speed of lateral overturning during a turn include the tractor weight, turning radius, mass center location, wheelbase, and track width.

2.1.3. Backward Rollover While Driving on Slope

Figure 3 shows a diagram for analyzing the backward rollover of a rear wheel drive tractor traveling on a slope [19]. The diagram captures the relative motion between the main body, including the front and rear wheels, with the dotted lines indicating the body's rotation by $\theta$ relative to the $Y$-axis.
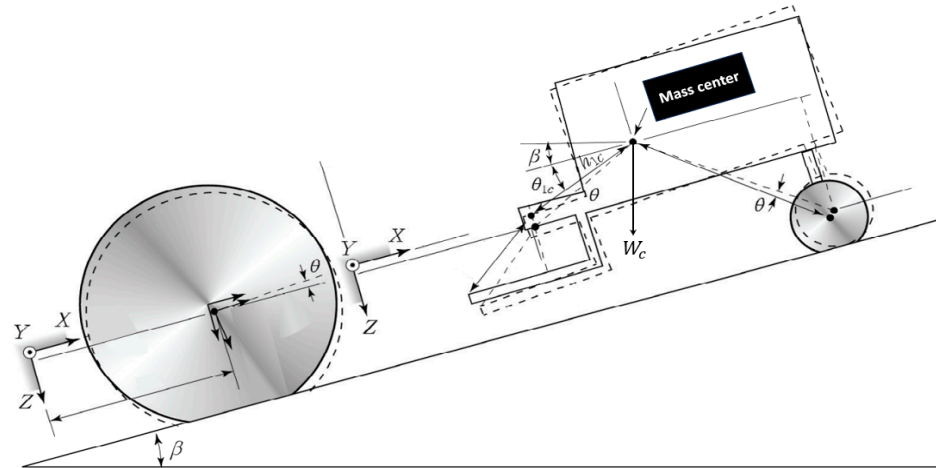


**Figure 3.** Diagram for backward rollover analysis.

As the angular acceleration $\ddot{\theta}$ and angular velocity $\dot{\theta}$ of the tractor increase, the risk of backward rollover caused by the rotation of the tractor's main body increases as well. If the angular velocity exceeds a certain threshold, then the tractor may rotate to a statically unstable angle, even without any driving torque or traction, thus resulting in a backward rollover. This occurs because when the angular velocity exceeds a certain value, the rotational kinetic energy promotes backward rollover. When the main body's rotation angle is $\theta_s$, the angular velocity that causes the tractor to rotate to this unstable angle is defined as the critical angular velocity $\dot{\theta}_s$, which can be obtained using Equation (6) [19]. A higher critical angular velocity indicates improved backward rollover safety.

$$\dot{\theta}_s = \sqrt{\frac{2W_c h_{1c}(1 - \sin[\theta_{1c} + \beta + \theta_s])}{I_{yyc} + m_c h_{1c}^2}}, \tag{6}$$

where $\dot{\theta}_s$ is the critical angular velocity for the backward rollover of the tractor, $m_c$ is the mass of the tractor body including the front wheels, $h_{1c}$ is the distance between the rear wheel center and mass center of the tractor, $\beta$ is the ground slope angle, $\theta_{1c}$ is the angle between the straight line of $h_{1c}$ and the $X$-axis, $\theta_s$ is the rotation angle of the tractor body, $W_c$ is the weight of the tractor body, and $I_{yyc}$ is the mass moment of inertia of the tractor body about the $Y$-axis passing through the mass center.

In Equation (6), the mass moment of inertia $I_{yyc}$ is determined by the tractor's mass center location, geometry, and weight distribution. The variables $h_{1c}$ and $\theta_{1c}$ are determined by the rear-axle height and mass center location. Therefore, the critical factors affecting the critical angular velocity for backward rollover when the tractor is on a slope include the tractor's main body weight, ground slope angle, rear-axle height, mass center location, weight distribution, and geometric shape.

2.1.4. Analysis of Factors That Affect Lateral Overturning and Backward Rollover of Wheeled and Tracked Tractors

The theoretical analysis identified several factors influencing lateral overturning and backward rollover: tractor weight, track width, wheelbase, mass center location, weight distribution, heights of the front and rear axles, and geometric shape (Table 1).

**Table 1.** Factors affecting tractor overturning and rollover.

| Items | Influencing Factors |
|---|---|
| Lateral overturning in stationary state | Wheelbase<br>Track width<br>Location of mass center<br>Front-axle height |
| Lateral overturning in steady state turning | Mass<br>Location of mass center<br>Wheelbase<br>Track width |
| Backward rollover in traveling on slopes | Mass<br>Location of mass center<br>Rear-axle height<br>Weight distribution<br>Geometric shape |
| Total | Mass<br>Wheelbase<br>Track width<br>Location of mass center<br>Front-axle height<br>Rear-axle height<br>Weight distribution<br>Geometric shape |

The theoretical analysis is discussed based on a wheeled tractor owing to the dearth of studies related to tracked tractors; however, the mass, mass center location, weight distribution, and geometric shape can be equally applied to tracked tractors. The wheelbase is defined as the straight distance between the centers of the front and rear axles for wheeled tractors but is the length of the ground contact region for tracked tractors [22]. For wheeled tractors, the wheels are elements that rotate the tires via power transmitted from the engine. In tracked tractors, components such as the sprocket, idler, and roller that rotate the track serve a similar function to the wheels. Therefore, the axle height of wheeled tractors can be equated to the height of the sprocket, idler, and roller in tracked tractors. The track width refers to the distance between the wheels on a wheeled tractor, whereas it refers to the distance between the tracks on a tracked tractor. The track width of a tracked tractor is different from that of a wheeled tractor in that the front and rear lengths of the track width are the same. Wheeled and tracked tractors have similar overall configurations except for driving devices, and the results of the theoretical analysis show that factors affecting wheeled tractors are physical properties that are applicable to tracked tractors. Therefore, theoretical analysis of wheeled tractors can be similarly applied to tracked tractors (Table 2).

**Table 2.** Application of influencing factors from wheeled tractors to tracked tractors.

| Items | Wheeled Tractors | Tracked Tractors |
|---|---|---|
| Wheelbase | Straight distance between centers of front and rear axles | Length of ground contact region |
| Height of front and rear axles | Height of front and rear axles | Height of sprocket, idler, and roller |
| Track width | Different distances between front and rear regions | Same distance between front and rear regions |

To accurately implement the overturning and rollover characteristics of an actual tractor, one must ensure that the influencing factors listed in Table 1 are accurately reflected in the simulation model. Among these factors, the tractor weight, track width, wheelbase, and the heights of the front and rear axles can be derived through straightforward measure-

ments. However, determining the mass center location requires a more complex procedure that adheres to an international standard.

### 2.2. Miniature Tracked Forestry Tractor

A miniature tracked forestry tractor scaled down to 1:11 of the actual size was used in the tests. The model's maximum driving speed is 0.52 km/h, which is achievable in both forward and reverse motion, and it was controlled using a remote controller. The miniature tracked forestry tractor is the NST-1500VD model manufactured by Mitsubishi in Japan. Its main body was made of alloy steel and stainless steel, whereas its tracks were made of aluminum alloy. The geometry and specifications of the miniature tracked forestry tractor are shown in Figure 4 and Table 3, respectively.



**Figure 4.** Photograph of miniature tracked forestry tractor.

**Table 3.** Specifications of miniature tracked forestry tractor.

| Items | | Specifications |
|---|---|---|
| Model | | NST-1500VD |
| Length/width/height (mm) | | 515/220/240 |
| Weight (kg) | | 13.30 |
| Maximum lifting weight (kg) | | 15 |
| Material | | Alloy steel, stainless steel, aluminum alloy |
| Maximum traveling | Forward | 0.52 |
| speed (km/h) | Backward | 0.52 |

Mass Center Derivation

Determining the mass center location requires a more complex test compared with the case for the other factors. The mass center location of the miniature model was derived from an experiment conducted in accordance with the International Organization for Standardization 789-6:2019 [23], which specifies the procedure for determining the mass center of a tracked tractor.

This process involved measuring the combined reaction forces of the tractor, deck, and knife edges ($F_1 + F_2$) using a weighing machine. Subsequently, the front reaction force of the deck and knife edges alone ($F_1$) was measured. The tractor's specific contribution to the front section's reaction force ($F_2$) was derived from the difference between these two measurements. Subsequently, the horizontal coordinate of the mass center was calculated using ($F_2$), the total weight of the tractor (W), and the distance between the front and rear knife edges (d), as shown in Equation (7) (Figure 5).

$$\bar{x} = \frac{d \cdot F_2}{W},$$ (7)

where $\bar{x}$ is the horizontal distance of the mass center from the rear knife edge, W is the total weight of the tracked tractor, d is the distance between the front and rear knife edges, and $F_2$ is the reaction force by the tracked tractor weight at the front knife edge.
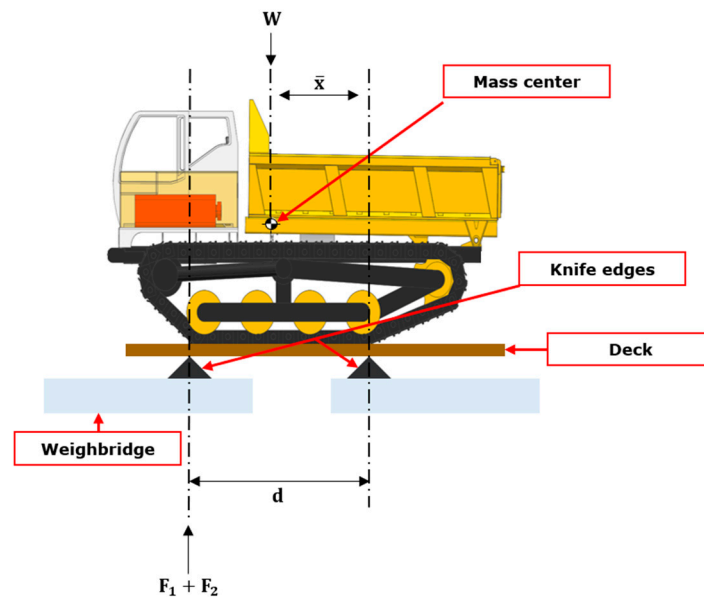


**Figure 5.** Diagram to determine horizontal location of mass center.

The vertical coordinate of the mass center can be determined using Equations (8) and (9), which involve the total weight of the tractor, the reaction force at the knife edge, and the horizontal distance from the knife edge to the cable (Figure 6). Initially, the rear end of the tractor track was positioned on the knife edge, and the reaction force at this point was measured, whereas the front end of the tractor was lifted to an angle between 20° and 25° using the front cable. The horizontal distance from the front cable to the knife edge ($d_1$) was measured, and the horizontal distance from the front cable to the mass center ($c_1$) was derived using Equation (8). Subsequently, a vertical line was drawn from the cable at a horizontal distance of $c_1$. Similarly, after locating the front end of the tractor track on the knife edge, the horizontal distance from the rear cable to the knife edge ($d_2$) was measured when the rear end of the tractor was lifted. The horizontal distance from the rear cable to the mass center ($c_2$) was derived using Equation (9). A vertical line was drawn at a horizontal distance of $c_2$ from the cable, and the intersection of these vertical lines from $c_1$ and $c_2$ determines the vertical coordinate of the mass center ($\bar{h}$).

$$c_1 = \frac{F_3 \cdot d_1}{W} \tag{8}$$

$$c_2 = \frac{F_4 \cdot d_2}{W}, \tag{9}$$

where $c_1$ is the horizontal distance of the mass center from the front end cable, $c_2$ is the horizontal distance of the mass center from the rear end cable, $F_3$ is the reaction force at the rear knife edge when lifting the front end of the tracked tractor, $F_4$ is the reaction force at the front knife edge when lifting the rear end of the tracked tractor, $d_1$ is the horizontal distance from the front cable to the rear knife edge, and $d_2$ is the horizontal distance from the rear cable to the front knife edge.
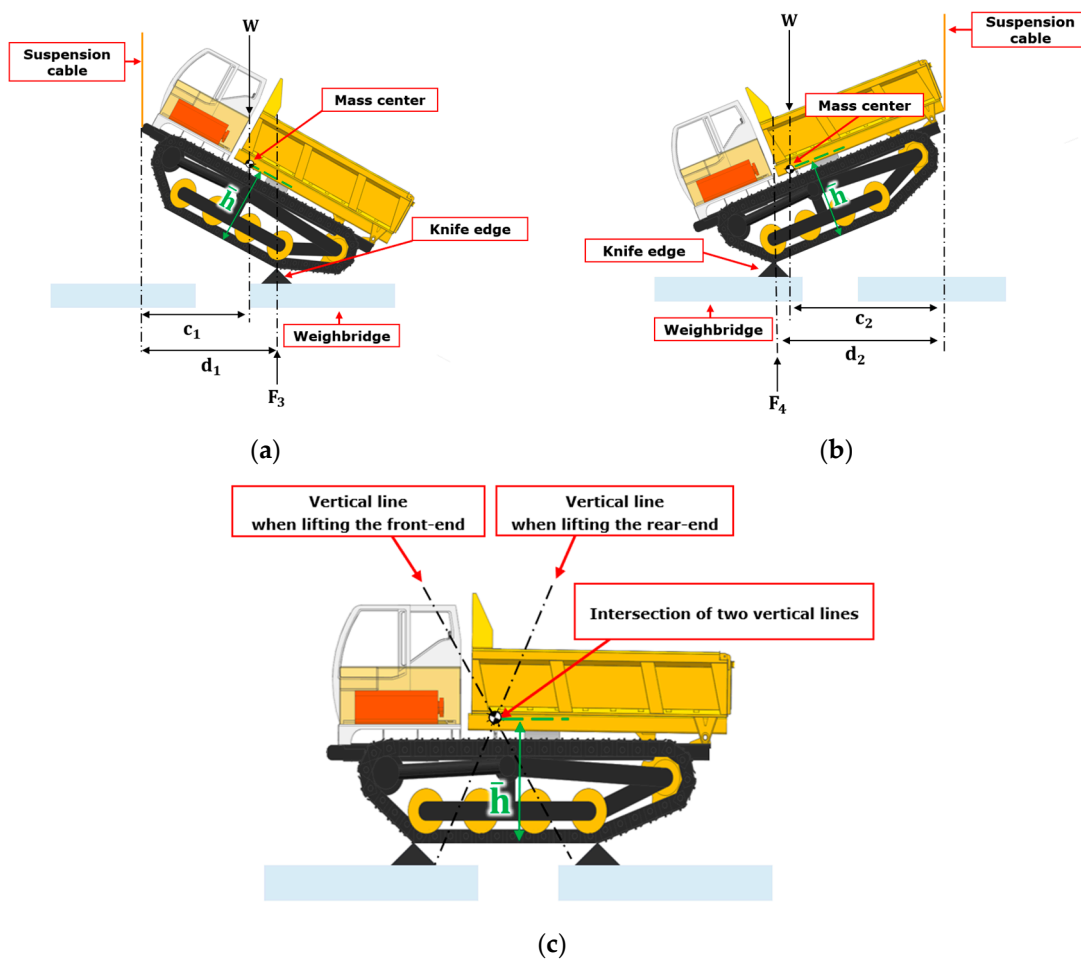
**Figure 6.** Diagram to determine vertical location of mass center: (**a**) lifting of front end; (**b**) lifting of rear end; (**c**) intersection of two vertical lines.

The lateral coordinate of the mass center was derived from the total weight of the tractor, the reaction force of the right track, and the track width (Figure 7). The reaction force of the right track and the track width were initially measured and then used in Equation (10) to calculate the offset of the mass center (b). Subsequently, the lateral coordinate of the mass center was derived using this offset and the track width (Equation (11)).

$$b = \frac{F_5 \cdot d_t}{W} \tag{10}$$

$$\bar{y} = \frac{d_t}{2} - b, \tag{11}$$

where $\bar{y}$ is the lateral location of the mass center from the center of two tracks, b is the lateral offset between the mass center and left track center, $F_5$ is the reaction force at the right-side tracks, and $d_t$ is the track width.
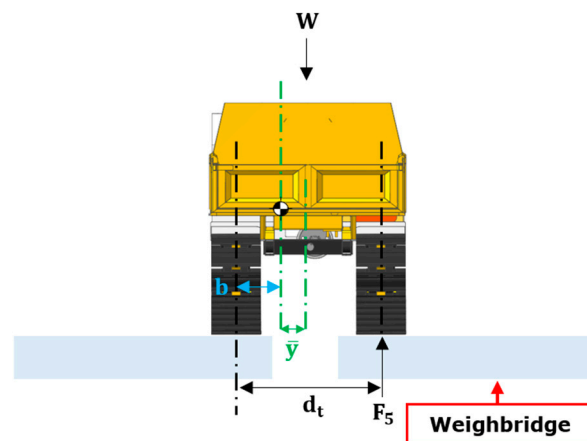
**Figure 7.** Diagram to determine lateral location of mass center.

*2.3. Three-Dimensional (3D) Simulation Model*

2.3.1. Three-Dimensional Model Construction

The 3D model of the miniature tractor was constructed by accurately reflecting all the factors affecting overturning and rollover. For this model, the measurements from the actual tractor were applied for the total weight, track width, wheelbase, height of the front and rear axles, and geometric shape. The experimentally derived value for the mass center location was incorporated as well. Additionally, the material properties of each element of the actual tractor were considered. The exterior of the miniature tracked forestry tractor was made of stainless steel, whereas the internal components, such as the hydraulic cylinder, motor, sprocket, idler, and roller, were made of alloy steel. The track was crafted from aluminum alloy. Table 4 shows the properties of the materials used [24]. To ensure an efficient and simple simulation, the smaller components inside the tractor (e.g., breadboard, wires, and MCU) were replaced with a mass cube [25,26]. The weight and position of this mass cube were adjusted to ensure that the 3D model's total weight and mass center location precisely matched those of the miniature tracked forestry tractor.

**Table 4.** Material properties of miniature tracked forestry tractor used in simulation.

| Items | | Value |
|---|---|---|
| Stainless steel (main body frame) | Poisson's ratio | 0.3 |
| | Elastic modulus (GPa) | 180 |
| | Density (kg/m$^3$) | 7930 |
| Alloy steel (hydraulic cylinder, motor, sprocket, idler, and roller) | Poisson's ratio | 0.3 |
| | Elastic modulus (GPa) | 210 |
| | Density (kg/m$^3$) | 1900 |
| Aluminum alloy (track) | Poisson's ratio | 0.33 |
| | Elastic modulus (GPa) | 71 |
| | Density (kg/m$^3$) | 2700 |

2.3.2. Verification of Simulation Model

A simulation model utilizing the developed 3D model was constructed using commercial dynamic simulation software (Recurdyn 2023, Function Bay, Seongnam, Republic of Korea). To determine whether this model accurately represents the overturning and rollover characteristics of the actual tractor, it was verified based on the static sidelong falling angle and minimum turning radius.

Static Sidelong Falling Angle

The static sidelong falling angle test, an official method for assessing tractor safety, involves incrementally increasing the slope angle from 0° to 90°. During this test, a slope

with a high friction coefficient is used to prevent slippage between the wheels and surface. The angle at which the upslope wheel or track lifts off the surface is recorded as the static sidelong falling angle [20].

To simulate the static sidelong falling angle test of an actual tractor, a test platform comprising a digital level, sloping plate, fixed plate, rubber pad, cable, and cushion (to prevent shock prevention) was set up (Figure 8). The digital level (Advanced digital level, YATO, Seoul, Republic of Korea) was used to measure the angle of the sloping plate. The rubber pad was fixed on the sloping plate to prevent track slippage. The cable, which was attached to the sloping plate through holes drilled at its upper and lower ends, was used to lift the plate quasi-statically. The cushion was installed on the fixed plate to protect against damage if the tractor overturns during the test. The sloping and fixed plates, which were made of wood and connected by hinges, allowed for the adjustment of the slope angle. During the test, the slope angle was increased gradually at increments of 0.01°, and the angle at which the upslope track lifted off the surface was measured. The test was repeated five times to ensure accuracy, and a high-speed camera (DC-GH5, Panasonic, Osaka, Japan) was used to capture the process and verify the precise angle.
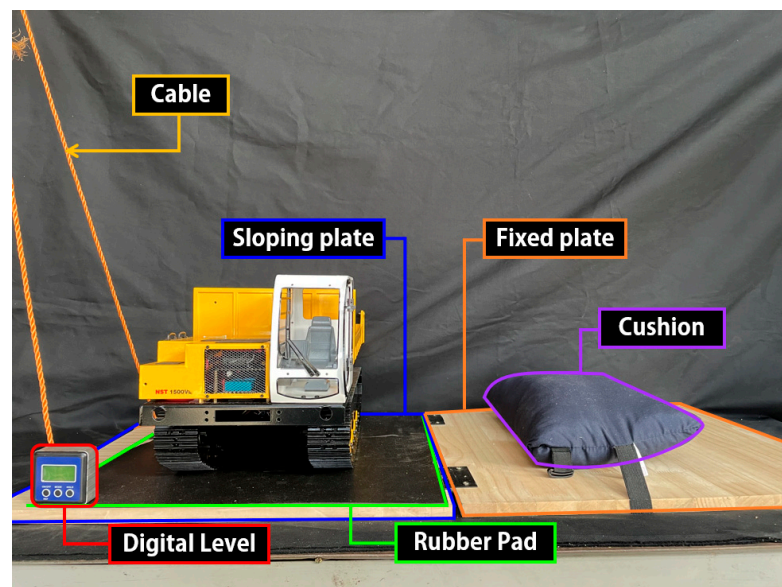


**Figure 8.** Platform established to perform static sidelong falling angle test.

A simulation model that simulates the static overturning characteristics of an actual tractor was developed. In this model, a 3D model tractor was placed on a slope, and the slope angle was increased at intervals of 0.01°, as performed in real-world testing, to determine the angle at which the reaction force of the upslope track becomes zero. The properties related to the track-ground contact—stiffness, friction, and damping coefficients—were selected based on a previous study [27] and are detailed in Table 5. These conditions were selected to prevent sideslip between the ground and track, thus reflecting the actual test.

**Table 5.** Properties used in static sidelong falling angle simulation.

|  | Items | Value |
|---|---|---|
| | Stiffness coefficient (N/mm) | $10^8$ |
| Interaction between | Damping coefficient (N·s/mm) | $10^4$ |
| track and ground | Coefficient of dynamic friction | 1.5 |
| | Coefficient of static friction | 1.85 |

Minimum Turning Radius

The turning radius is another critical factor affecting the overturning and rollover characteristics of a tractor. A smaller turning radius enhances work efficiency by facilitating easier steering and access to confined spaces [28]. The minimum turning radius test, which is recognized as an official test, defines the tracked tractor's minimum turning radius as the radius of the trajectory drawn by the center of the outer track when the tractor turns at a speed not exceeding 2 km/h in a counterclockwise direction, with the left track propagating backward and the right track forward.

For the miniature tracked forestry tractor, the speed was set to a minimum value of 0.04 km/h, which reflects the actual minimum turning radius used in the test. The tractor was maneuvered with the right track propagating forward and the left track backward, and the trajectory radius drawn by the center of the right track was measured.

Additionally, a simulation model capable of simulating the minimum turning radius of the actual tractor was developed. This model used the same speeds and track directions as the actual test. It calculated the trajectory radius of the right track's center during the turn.

The static sidelong falling angle test was conducted in a state where sideslip did not occur; therefore, extremely large stiffness and damping coefficients were applied to prevent sideslip from occurring in the simulation. However, sideslip occurred in the minimum turning radius test; therefore, realistic levels of stiffness and damping coefficients were applied in the simulation [29]. This aspect was integrated into the dynamic simulation, and the ground contact properties were specified accordingly (Table 6).

**Table 6.** Properties used in minimum turning radius simulation.

| Items | | Value |
|---|---|---|
| | Stiffness coefficient (N/mm) | $10^3$ |
| Interaction between | Damping coefficient (N·s/mm) | 0.5 |
| track and ground | Coefficient of dynamic friction | 1.2 |
| | Coefficient of static friction | 1.55 |

## 3. Results and Discussions

### 3.1. Mass Center Derivation Results for Miniature Tracked Forestry Tractor

The horizontal coordinate of the mass center was 157.9 mm from the rear knife edge of the tractor in the forward direction (Figure 9). As the distance from the rearmost section of the tractor to the rear knife edge was 125 mm, the mass center in the horizontal direction was located at 282.9 mm from the rearmost section. Because the total length of the miniature tractor was 515 mm, the mass center was located toward the front section, likely due to the placement of heavier components, such as the battery and hydraulic cylinder, in this area.

The vertical coordinate of the mass center was situated 102 mm above the ground (Figure 10). As the total height of the tractor was 240 mm, the mass center was positioned relatively low, which can be attributed to the location of heavier elements, such as the track and hydraulic cylinder, in the lower section of the tractor.

The lateral coordinate of the mass center was 1.4 mm off-center, which shifted toward the driver's seat from the midpoint between the left and right tracks (Figure 11). That the width of the tractor was 220 mm indicates that the mass center was almost centrally located within the tractor's width.
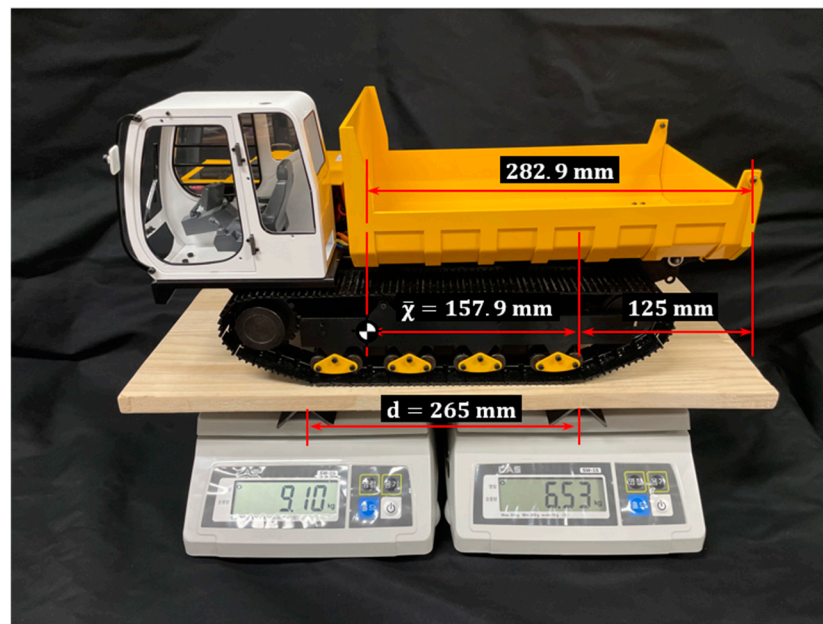
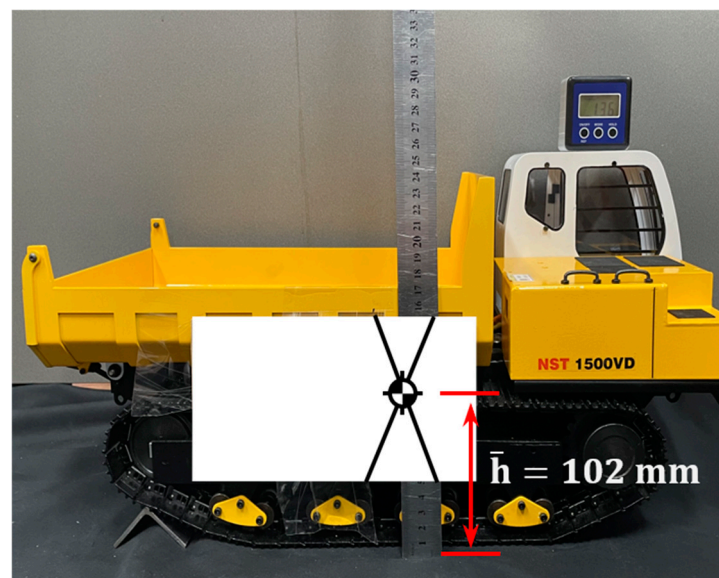**Figure 9.** Horizontal location of mass center for miniature tracked forestry tractor.



**Figure 10.** Vertical location of mass center for miniature tracked forestry tractor.

### 3.2. 3D Modeling Results for Miniature Tracked Forestry Tractor

The 3D model was constructed to replicate the geometric shape, track width, wheelbase, and axle height of the actual miniature tracked forestry tractor (Figure 12). Comparisons between the 3D model and the actual tractor showed track width and wheelbase error rates of 0.78% and 1.02%, respectively (Table 7). The error rates for the total weight and the weight distribution between the left and right tracks were both 0%, thus indicating that the developed 3D model accurately simulated these aspects of the actual tractor (Table 8).
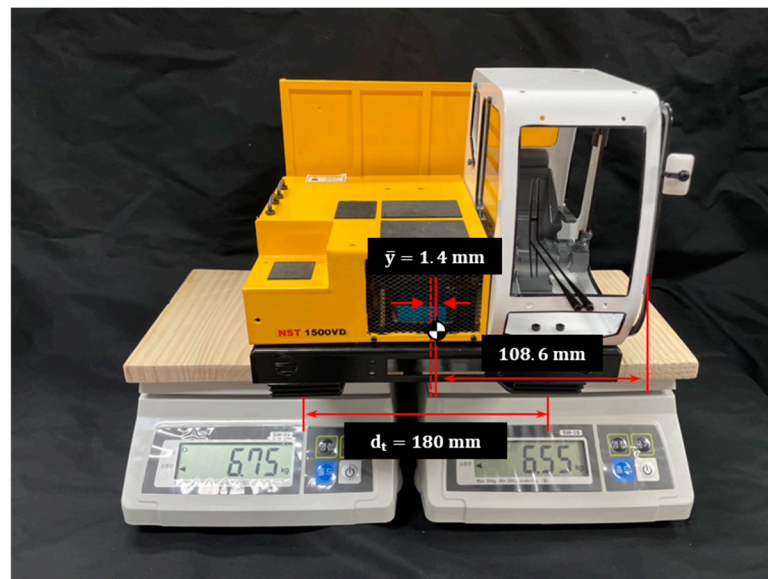
**Figure 11.** Lateral location of mass center for miniature tracked forestry tractor.
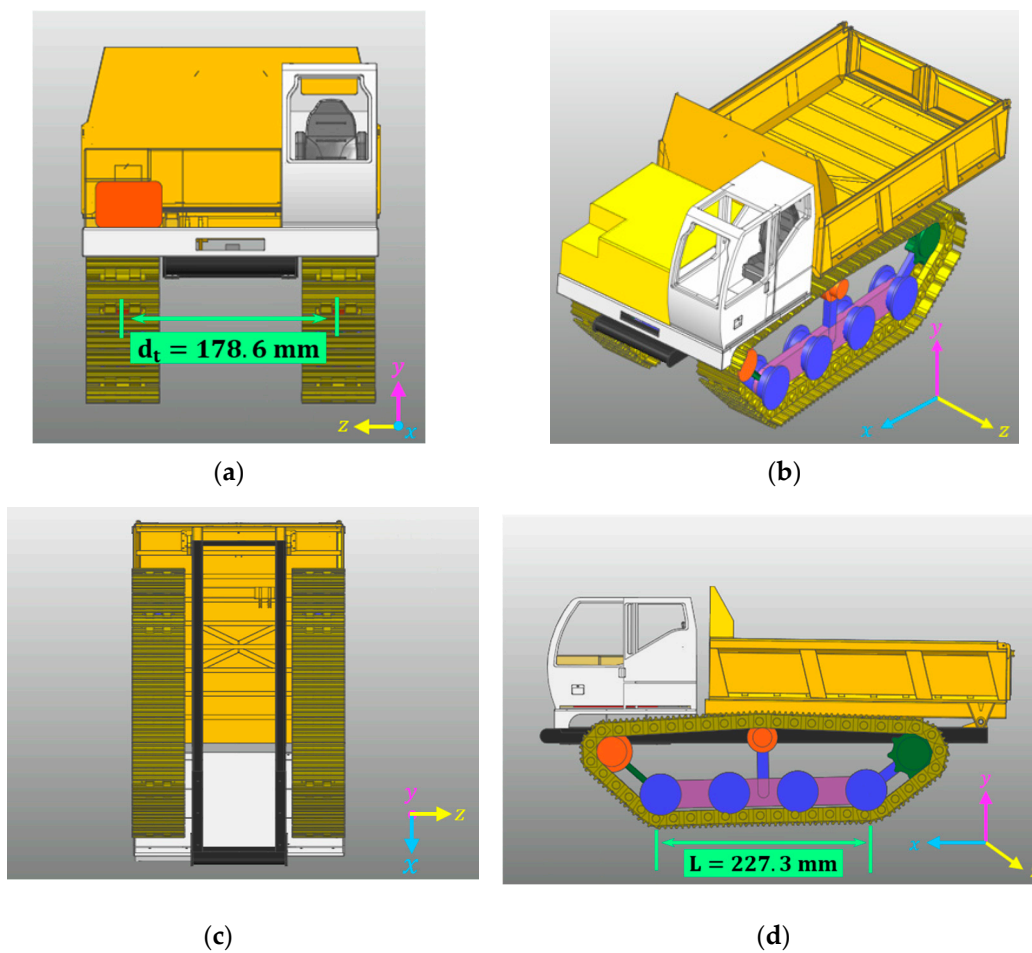


(**a**)

(**b**)

(**c**)

(**d**)

**Figure 12.** Three-Dimensional model of miniature tracked forestry tractor: (**a**) front view; (**b**) isometric view; (**c**) bottom view; (**d**) side view.

**Table 7.** Comparison of track width and wheelbase.

| Items | Track Width (mm) | Wheelbase (mm) |
|---|---|---|
| Actual tractor | 180.0 | 225.0 |
| 3D model | 178.6 | 227.3 |
| Error rate (%) | 0.78 | 1.02 |

**Table 8.** Comparison of total weight and weight distribution.

| Items | Total Weight (kg) | Weight Distribution (kg) | |
|---|---|---|---|
| | | Left Track | Right Track |
| Actual tractor | 13.30 | 6.55 | 6.75 |
| 3D model | 13.30 | 6.55 | 6.75 |
| Error rate (%) | 0 | 0 | 0 |

The mass center location in the developed 3D model was derived (Figure 13) and compared with that of the actual tractor. The error rates for the horizontal, vertical, and lateral coordinates of the mass center were 0.2%, 0.1%, and 1.1%, respectively, thus confirming that the 3D model closely simulated the mass center of the actual tractor (Table 9).
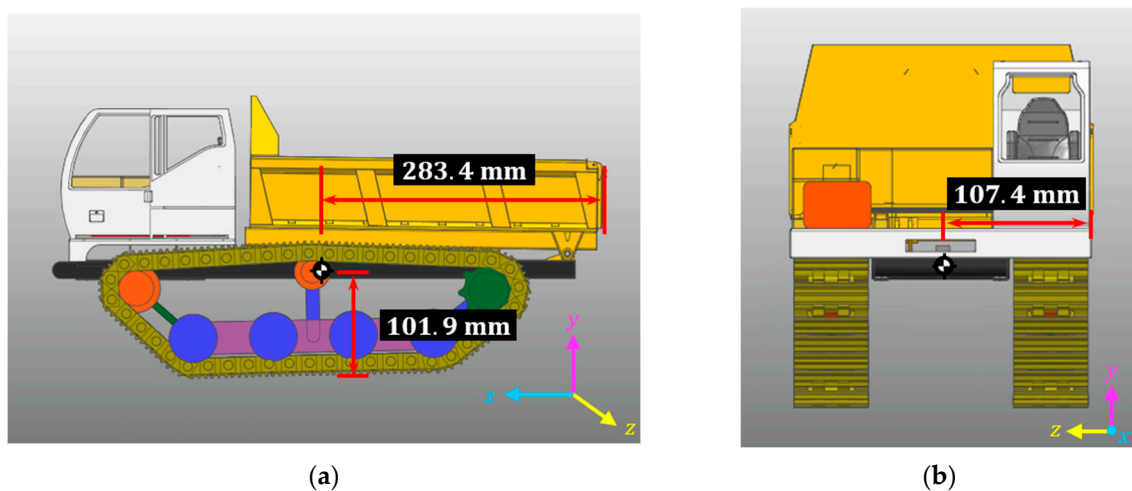


**Figure 13.** Position of mass center in 3D model: (**a**) side view; (**b**) front view.

**Table 9.** Comparison of mass center positions.

| Items | Coordinate (mm) | | |
|---|---|---|---|
| | Horizontal | Vertical | Lateral |
| Actual tractor | 282.9 | 102.0 | 108.6 |
| 3D model | 283.4 | 101.9 | 107.4 |
| Error rate (%) | 0.2 | 0.1 | 1.1 |

The 3D model was designed to fully reflect the geometric shape of the actual tractor. The error rates for the track width, wheelbase, total weight, weight distribution, and mass center location were all below 5%, thus demonstrating that the model can accurately simulate the overturning and rollover characteristics of the actual tractor with high accuracy because it accurately reflected all factors affecting the overturning and rollover of the actual tractor.

### 3.3. Simulation Model Verification Results

Figure 14 shows the practical test and simulation results for the static sidelong falling angle of the miniature tracked forestry tractor. The average static sidelong falling angle was recorded as 50.30° based on five repeated measurements and 51.7° in the simulation, thus resulting in an error rate of 2.73% (Table 10). As the error rate was under 5%, one may conclude that the developed simulation model effectively simulated the static overturning characteristics of the actual tractor.



(**a**)                                         (**b**)

**Figure 14.** Practical test and simulation of static sidelong falling angle test: (**a**) practical test; (**b**) simulation.

**Table 10.** Error rate of static sidelong falling angle between practical test and 3D simulation.

| Item | Static Sidelong Falling Angle (°) |
|---|---|
| Practical test | 50.3 |
| Simulation | 51.7 |
| Error rate (%) | 2.73 |

Figure 15 shows the practical test and simulation results for the minimum turning radius of the miniature tracked forestry tractor. The average minimum turning radius was 163.14 mm in the test and 162.19 mm in the simulation, which resulted in an error rate of 0.58% (Table 11). As the error rate was below 5%, one may conclude that the developed simulation model accurately simulated the turning characteristics of the actual tractor.
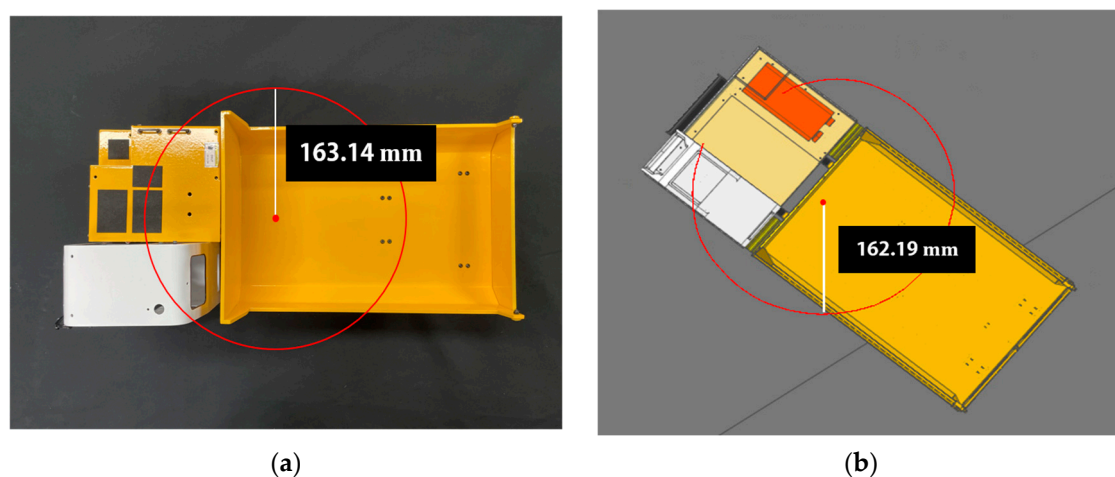


(**a**)                                         (**b**)

**Figure 15.** Practical test and simulation of minimum turning radius: (**a**) practical test; (**b**) simulation.

**Table 11.** Error rate of minimum turning radius between practical test and 3D simulation.

| Item | Minimum Turning Radius (mm) |
|---|---|
| Practical test | 163.14 |
| Simulation | 162.19 |
| Error rate (%) | 0.58 |

The developed simulation model accurately replicated the static overturning and turning radius characteristics of the actual tractor. This high level of accuracy is attributed to the comprehensive incorporation of critical factors such as the total weight, weight distribution, and the location of the mass center into the 3D model. Therefore, if a 3D model is constructed and simulations are performed using the method proposed in this study, then one can expect the overturning and rollover characteristics of the actual tractor to be accurately predicted through simulation, thereby eliminating the necessity for physical testing. Future studies should focus on verifying the effectiveness of the simulation under varying ground and dynamic driving conditions to further enhance the model's applicability.

## 4. Conclusions

In this study, a simulation model that can accurately simulate the overturning and rollover characteristics of an actual tractor was developed and verified via testing. Influencing factors vital to the simulation's accuracy were derived through a theoretical analysis of tractor overturning and rollover dynamics. They were described based on wheeled tractors, as prior research pertaining to tracked tractors is not available; however, all the factors are applicable to tracked tractors. Among the factors, the mass center location was measured in accordance with the international standards, whereas the tractor's weight, track width, wheelbase, weight distribution, height of the front and rear axles, and geometric shape were derived through direct measurements. A 3D model was created to encompass all these factors. In this model, smaller components that did not affect the geometric shape were replaced with a mass cube. Comparisons between the 3D model and the actual tractor showed track width and wheelbase error rates of 0.78% and 1.02%, respectively. Errors in the weight and the distribution of weight between the left and right tracks were negligible (0%). The error rates for the coordinates of the mass center between the 3D model and the actual tractor were under 5%, thus demonstrating that the 3D model precisely represented the actual tractor.

The dynamic simulation model, which incorporated the developed 3D model, was verified based on the static sidelong falling angle and minimum turning radius through tests. For these characteristics, the error rates derived from comparisons with the actual tractor, based on the averages of five repeated measurements, were 2.73% and 0.58%, respectively. As these error rates were below 5%, the model was confirmed to effectively replicate the overturning and rollover characteristics of the actual tractor. This indicates that a simulation model constructed using this method can reliably emulate the physical attributes and behavior of actual tractors, i.e., physical tests are not necessitated.

**Data Availability Statement:** The original contributions presented in the study are included in the article, further inquiries can be directed to the corresponding author.

**Conflicts of Interest:** The authors declare no conflicts of interest.

## References

1. Shin, Y.S.; Youn, K.W.; Kim, K.S.; Choi, D.P.; Hong, S.J.; Lee, M.J. Characteristics and prevention measures of traffic accidents causing injuries to agricultural machinery occupants in the Jeonnam region. *JKDAS* **2023**, *25*, 1577–1595. [CrossRef]
2. Koh, J.W.; Kwon, S.C.; Kim, K.R.; Lee, K.S.; Jang, E.C.; Kwon, Y.J.; Ryu, S.H.; Lee, S.J.; Song, J.C. A study on the development of surveillance system for agricultural injuries in Korea. *J. Agric. Med. Community Health* **2007**, *32*, 139–153. [CrossRef]
3. Sohn, J.R.; Park, J.H.; Kim, S.P.; Kim, S.J.; Cho, S.H.; Cho, N.S. Analysis of risk factors influencing the severity of agricultural machinery related injuries. *JKSEM* **2007**, *18*, 300–306.
4. Kim, S.J.; Gim, D.H.; Jang, M.K.; Hwang, S.J.; Yang, Y.J.; Nam, J.S. Development of regression model for predicting the maximum static friction force of tractors with a front-end loader. *J. Biosyst. Eng.* **2023**, *48*, 329–338. [CrossRef]
5. Jeong, C.W.; Kim, D.J. A Study on the disaster analysis and accident prevention measures for agricultural work. *Korean J. Hazard. Mater.* **2023**, *11*, 50–57. [CrossRef]
6. Togaev, A.; Shermukhamedov, A. Tractor rollover accidents: A review of factors and safety measures. *E3S Web Conf.* **2023**, *449*, 09011. [CrossRef]
7. Facchinetti, D.; Santoro, S.; Galli, L.E.; Pessina, D. Agricultural tractor roll-over related fatalities in Italy: Results from a 12 years analysis. *Sustainability* **2021**, *13*, 4536. [CrossRef]
8. Previati, G.; Gobbi, M.; Mastinu, G. Mathematical models for farm tractor rollover prediction. *J. Veh. Design.* **2014**, *64*, 280–303. [CrossRef]
9. Franceschetti, B.; Rondelli, V.; Ciuffoli, A. Comparing the influence of roll-over protective structure type on tractor lateral stability. *Saf. Sci.* **2019**, *115*, 42–50. [CrossRef]
10. Lee, D.G.; Yoo, H.J.; Shin, M.J.; Oh, J.S.; Shim, S.B. Analysis of overturning stability of small off-road vehicle. *J. Biosyst. Eng.* **2023**, *48*, 309–318. [CrossRef]
11. Kim, Y.S.; Lee, S.D.; Kim, Y.J.; Kim, Y.J.; Choi, C.H. Effect of tractor travelling speed on a tire slip. *KJOAS* **2018**, *45*, 120–127. [CrossRef]
12. Shim, S.B.; Park, Y.J.; Kim, K.U.; Kim, J.W.; Park, M.S.; Song, T.Y. Computer simulation of sideways overturning of side-loaded mini forwarder. *J. Biosyst. Eng.* **2007**, *32*, 69–76. [CrossRef]
13. Kang, S.H.; Kim, J.H.; Kim, Y.S.; Woo, S.M.; Daniel, D.U.; Ha, Y.S. A simulation study on the dynamics characteristics of hot pepper harvester. *J. Korean Soc. Simul.* **2020**, *29*, 19–25. [CrossRef]
14. Iqbal, M.Z.; Islam, M.N.; Ali, M.; Kiraga, S.; Kim, Y.J.; Chung, S.O. Theoretical overturning analysis of a 2.6-kW two-row walking-type automatic pepper transplanter. *J. Biosyst. Eng.* **2022**, *47*, 79–91. [CrossRef]
15. Park, H.K.; Kim, K.U.; Kim, J.W.; Song, T.Y.; Park, M.S.; Cho, K.H. Sideways overturning analysis of forwarder using a multibody dynamics analysis program. *J. Biosyst. Eng.* **2002**, *27*, 185–194. [CrossRef]
16. Qin, J.; Zhu, Z.; Ji, H.; Zhu, Z.; Li, Z.; Du, Y.; Song, Z.; Mao, E. Simulation of active steering control for the prevention of tractor dynamic rollover on random road surfaces. *Biosyst. Eng.* **2019**, *185*, 135–149. [CrossRef]
17. Eom, B.G.; Kang, B.B.; Lee, H.S. A running stability test of 1/5 scaled bnogie using small-scaled derailment simulator. *KISTI* **2012**, *15*, 9–16. [CrossRef]
18. Carson, J.S. Introduction to modeling and simulation. *Johns Hopkins APL Tech. Dig.* **1995**, *12*, 6–17.
19. Shin, B.S.; Kim, D.C.; Kim, Y.J.; Kim, H.J.; Nam, J.S.; Park, Y.J.; Shim, S.B.; Lee, D.H.; Lee, J.W.; Cho, Y.J.; et al. *Tractor Engineering Principles*, 2nd ed.; Moon Woon Dang: Seoul, Republic of Korea, 2021.
20. Jang, M.K.; Hwang, S.J.; Shin, C.S.; Nam, J.S. A novel approach to determine static falling down sidelong angle of tractor using a 3D printed miniature model. *Appl. Sci.* **2021**, *12*, 43. [CrossRef]
21. Baker, V.; Guzzomi, A.L. A Model and Comparison of 4-wheel-drive fixed-chassis tractor rollover during Phase 1. *Biosyst. Eng.* **2013**, *116*, 179–189.
22. *No. 2017–668*; Performance of Automobiles and Automobile Parts and Detailed Rules for Implementation of Standards. Ministry of Land, Infrastructure and Transport: Sejong-si, Republic of Korea, 2017.
23. *No. 789-6:2019*; Agricultural Tractors-Test Procedures-Part 6: Centre of Gravity. ISO: Geneva, Switzerland, 2019.
24. Khot, S.S.; Navthar, R.R. Design and optimization of front axle of heavy truck. *IJEAST* **2019**, *4*, 183–191. [CrossRef]
25. Kim, T.J.; Jeon, H.H.; Kim, Y.J. Dynamic characteristic analysis of an autonomous tractor according to plow tillage. *PASTJ* **2019**, *1*, 56. [CrossRef]
26. Lysych, M.N. Study driving dynamics of the machine-tractor unit on a virtual stand with obstacles. *J. Phys. Conf. Ser.* **2020**, *1515*, 042079. [CrossRef]
27. Jeong, H.J.; Yu, J.W.; Lee, D.H. Track HM design for dynamic analysis of 4-tracked vehicle on rough terrain using Recurdyn. *Trans. Korean Soc. Mech. Eng. A* **2021**, *45*, 275–283. [CrossRef]

28. Kim, Y.Y.; Lim, G.K.; Shin, S.Y.; Kim, H.J.; Kim, B.G.; Kim, H.G. Development of a turning radius measurement system using DGPS for agricultural tractors. *J. Biosyst. Eng.* **2010**, *35*, 85–90. [CrossRef]
29. Wang, Y.; Yang, F.; Pan, G.; Liu, H.; Liu, Z.; Zhang, J. Design and testing of a small remote-control hillside tractor. *Trans. ASABE* **2014**, *57*, 363–370. [CrossRef]